Interactions of solitary waves in the Adlam-Allen model

Boris A. Malomed [1,2] Panayotis G. Kevrekidis [3] Vassilis Koukouloyannis [4] Nathaniel Whitaker [3]
and Dimitrios J. Frantzeskakis [5]

[1]*Department of Interdisciplinary Studies, Faculty of Engineering, Tel Aviv University, Tel Aviv 69978, Israel*
[2]*Instituto de Alta Investigación, Universidad de Tarapacá, Casilla 7D, Arica, Chile*
[3]*Department of Mathematics Statistics, University of Massachusetts, Amherst, Massachusetts 01003-4515, USA*
[4]*Department of Mathematics, Laboratory of Applied Mathematics and Mathematical Modelling,*
University of the Aegean, Karlovasi, 83200 Samos, Greece
[5]*Department of Physics, National and Kapodistrian University of Athens, Panepistimiopolis, Zografos, Athens 15784, Greece*

We study the interactions of two or more solitary waves in the Adlam-Allen model describing the evolution of a (cold) plasma of positive and negative charges, in the presence of electric and transverse magnetic fields. In order to show that the interactions feature an exponentially repulsive nature, we elaborate two distinct approaches: (a) using energetic considerations and the Hamiltonian structure of the model, and (b) using the so-called Manton method. We compare these findings with results of direct simulations, and we identify adjustments necessary to achieve a quantitative match between them. Additional connections are made, such as with solitons of the Korteweg–de Vries equation. New challenges are identified in connection to this model and its solitary waves.

I. INTRODUCTION

The field of nonlinear plasma physics has been a rich source of intriguing problems for the dynamics of solitary waves in integrable and nearly integrable systems [1,2]. In particular, the famous work of Zabusky and Kruskal [3], which initiated the explosion of interest in solitons by showing that the continuum limit of the Fermi-Pasta-Ulam-Tsingou model [4,5] is the Korteweg–de Vries (KdV) equation [6], was a motivating theme for the work of Washimi and Taniuti [7]. The latter one demonstrated that small-amplitude ion-acoustic waves in plasmas are also governed by the KdV model; hence, solitonic excitations may be expected in this setting too. However, as indicated in the historical review of early studies of solitons [8], it was overlooked in the seminal works [3] and [7], and in the extensive literature initiated by them (see, e.g., Refs. [1,9,10]), that solitary waves were discovered in plasmas well before Refs. [3] and [7]. Indeed, a fundamental model put forth by Adlam and Allen in 1958 and 1960 [11,12] constitutes, arguably, one of the earliest encounters of the realm of plasma physics with the concept of solitary waves.

The analysis presented in Refs. [11] and [12] concerns the spatiotemporal evolution of the distribution of electrons and ions in a magnetized plasma. In this setting, the spatial variation occurs only along the x direction; the electric field acts in the (x, y) plane, being subject to the Faraday's and Gauss' laws; and the (transverse) magnetic field acting along the z direction obeys the Ampére's law. The Newtonian spatiotemporal dynamics of a plasma consisting of positive and negative charges is affected by the forces created by the electric and magnetic fields. In this framework, starting from first principles and utilizing well-established approximations, such

as the quasineutrality concept, a reduced system for plasma dynamics under the action of the electromagnetic field was derived [11,12]. Ultimately, the resulting Adlam-Allen (AA) system of partial differential equations (PDEs) involved only two evolution equations for the (rescaled) magnetic field B and the inverse density R, in the $(1 + 1)$-dimensional setting [11,12] (see Ref. [13] for a recent recount of the topic).

The AA system is the starting point of the present work. In particular, in a recent study [14] this nonlinear model of plasma physics was revisited, and key properties of its solutions, including solitary and periodic waves, were examined. In addition to that, a connection of the AA model to the KdV equation was established (see also Ref. [15]) through a multiscale reduction, and collisions of solitary waves were briefly addressed. In the present work, we aim to study interactions of solitary waves in the AA system in detail. It is well known that solitons in the KdV equation repel each other, and exact multisoliton solutions can be obtained by means of the inverse-scattering transform (IST) method [10,16,17]. Studies of interactions of solitary waves in nonintegrable models, relying upon the identification of their pairwise potential [18] or force [19], have been the subject of numerous studies; see, e.g., Ref. [20] for an early review of relevant results.

On the basis of the reduction of the AA model to the KdV equation for weakly supersonic speeds of the solitary waves [14], it is natural to expect repulsion between them in the AA system as well. However, the AA model does not have the integrable structure of the KdV, which provides exact multisoliton solutions; therefore, one needs to resort to asymptotic techniques, such as ones based on the Lagrangian and/or Hamiltonian structure of the model [18], or other methods which directly address the system of PDEs and related

conservation laws [19]. Here, we leverage both of these approaches and conclude that they lead to the *same* conclusions for the repulsion of the solitary waves. We then go on to corroborate analytical predictions by means of direct simulations.

The subsequent presentation is organized as follows. In Sec. II, we present the physical and mathematical basis of the above mentioned setup, including its Lagrangian and Hamiltonian structure and solitary-wave solutions. In Sec. III, we use the asymptotic form of the solitary waves and the Hamiltonian of the AA system to address the tail-tail interaction between solitary waves. In Sec. IV, we compare the predictions to numerical simulations and identify adjustments needed for a quantitative match between them. In Sec. V, we summarize our findings and highlight some directions for future studies. Finally, in Appendix A we provide an alternative systematic proof of our results for the interaction between solitary waves, by means of the so-called *Manton method* [19,21]. Appendix B offers a perspective on a different, but also important type of interaction, namely, that of a solitary wave with a localized defect.

II. THE MODEL, ITS PROPERTIES, AND SOLITARY WAVES

A. Introducing the AA model

The AA model introduced in Refs. [11,12] describes the wave propagation in a cold magnetized collisionless electron-ion plasma. In particular, it is assumed that the thermal motion is negligible in comparison to velocities of the particles due to the wave motion, and collisions are also neglected due to the fact that the collision frequencies are small (i.e., the mean time between collisions is much larger than the time that an ion or electron spends in the wave). Electrons and ions in the plasma are subject to the action of the magnetic field applied in the z direction, and there is an induced electric field in the y direction, while the assumption of the quasineutrality is consonant with the presence of a weak electric field in the x direction. The latter is true as long as the electron plasma frequency is much greater than the electron cyclotron frequency. Note that such a setting may find applications both in fusion research and in studies of astrophysical phenomena, such as the solar wind [22].

Adlam and Allen [11,12] described how a large-amplitude compressional magnetic-field pulse (or a train of pulses [14]) can exist and be sustained in the collisionless plasma. In particular, adopting the Lagrangian coordinate system (moving with the pulse), they have found a nonlinear solution of such a model involving ions, electrons, and the electric and magnetic fields. This solution corresponds to accumulation of the magnetic flux, which is sustained by the flow of the plasma across it. The particles' velocities must be large enough so that the ion Larmor radius is larger than the effective width D of the magnetic pulse and the electric field of the ions is able to pull the electrons across D. Then, D turns out to be $\sim c/\omega_p$, i.e., on the order of the collisionless skin depth (with c being the speed of light and ω_p the plasma frequency), and the strength of the magnetic pulse depends on the Alfvén Mach number M_A, which lies in the interval of $1 \leqslant M_A \leqslant 2$ (see, e.g., Refs. [23,24]).

The AA system can be expressed in the following dimensionless form [14] (see also Ref. [15]):

$$R_{tt} + \tfrac{1}{2}(B^2)_{xx} = 0, \tag{1}$$

$$B_{xx} - RB + R_0 B_0 = 0, \tag{2}$$

where the real functions $R(x, t) > 0$ and $B(x, t)$ represent, respectively, the inverse plasma density and the magnetic field, while constants R_0 and B_0 are the density and the magnetic field strength in the undisturbed plasma, respectively (note that if the plasma is assumed to be uniform and steady, then $B = B_0$ and $R = R_0$). These constants also set the boundary conditions at infinity, i.e., $R \to R_0$ and $B \to B_0$ as $|x| \to \infty$; notice that R_0 and B_0 are related by the following equation,

$$R_0 \equiv B_0^2 / C^2, \tag{3}$$

where C is the characteristic speed of small-amplitude waves propagating on top of the background solution $R = R_0$ and $B = B_0$. Details of the derivation and scaling of the AA system can be found in Refs. [11,12,14,15].

As mentioned above, Adlam and Allen have found a class of large-amplitude hydromagnetic solitary waves which propagate in this setting. Their analytical treatment was inherently nonlinear, due to the consideration of finite-amplitude waves and self-localization effects. Therefore, this treatment differs from that of linear waves commonly appearing in textbooks on plasma waves (see, e.g., Refs. [23,24]), according to which the (linear) small-amplitude waves are considered as weak perturbations propagating on top of a background equilibrium.

In this work, we focus on the fully nonlinear version of the AA model. The finite-amplitude solitary waves that we consider here share their qualitative properties with small-amplitude fast magnetoacoustic Alfvén modes, as obtained from the linear theory, under the approximation of the cold collisionless plasma [23,24]. In fact, these are compressional electromagnetic waves, propagating perpendicularly to the background magnetic field. The particle motion in the waves is in the direction transverse to the background magnetic field, with the electric and magnetic fields of the wave oriented perpendicular and parallel to the background magnetic field, respectively. The AA model describes the self-localization of the waves along the x direction perpendicular to the background magnetic field (which lies along the z direction). Furthermore, the Faraday's law, in conjunction with the presence of the magnetic field, accounts for the y component of the electric field, while the x component of the latter obeys the Gauss' law.

B. Solitary waves

It is convenient to eliminate the constant background from Eqs. (1) and (2) upon introducing the following definitions:

$$R(x, t) \equiv R_0 + u(x, t), \quad B(x, t) \equiv B_0 + w(x, t), \tag{4}$$

where the fields u and w satisfy vanishing boundary conditions at infinity, namely, $u, w \to 0$ as $|x| \to \infty$. Then, the respectively transformed Eqs. (1) and (2) read [14] as follows:

$$u_{tt} + \left(\tfrac{1}{2}w^2 + B_0 w\right)_{xx} = 0, \tag{5}$$

$$w_{xx} - R_0 w - B_0 u - uw = 0. \tag{6}$$

As shown in Ref. [14] (see also Ref. [25] for an earlier similar analysis), Eqs. (5) and (6) possess an exact solitary-wave solution of the following form:

$$w_{\text{sol}} = \frac{2B_0}{C} \frac{v^2 - C^2}{C + v \cosh\left(\frac{B_0\sqrt{v^2 - C^2}}{Cv}\xi\right)}, \qquad (7)$$

$$u_{\text{sol}} = -\frac{1}{v^2}\left(B_0 w_{\text{sol}} + \frac{1}{2}w_{\text{sol}}^2\right), \qquad (8)$$

$$\xi \equiv x - vt. \qquad (9)$$

Here, v is the solitary-wave's velocity, which takes values in the interval of

$$C < v < 2C. \qquad (10)$$

The lower bound C of v is set by the necessary condition for the existence of the homoclinic orbit that corresponds to the exact solitary-wave solution (this homoclinic orbit occurs in the phase plane of the dynamical system stemming from Eqs. (5) and (6) once traveling-wave solutions are sought). In terms of the underlying physics, this condition means that the nonlinear solitary waves propagate at speeds higher than the speed of the linear-wave propagation in the system [14]. On the other hand, the upper bound $2C$ for v in Eq. (10) follows from the requirement that the (inverse) density R must be positive definite. While formal solutions exist past this threshold, they have no physical meaning.

C. The Lagrangian and Hamiltonian structure

Here, we aim to reveal the Lagrangian and Hamiltonian structure of the AA system. For this purpose, following Ref. [26], it is relevant to define the potential $U(x, t)$ of field $u(x, t)$:

$$u \equiv \partial U/\partial x. \qquad (11)$$

The substitution of definition (11) in Eqs. (5) and (6) and subsequent integration of the former equation with respect to x replaces Eqs. (5) and (6) by the following equations:

$$U_{tt} + \left(\tfrac{1}{2}w^2 + B_0 w\right)_x = 0, \qquad (12)$$

$$w_{xx} - R_0 w - B_0 U_x - wU_x = 0, \qquad (13)$$

where we have set the constant of integration (which, in principle, may be a function of time) equal to zero, as per the assumption that $U(x)$ and $w(x)$ vanish as $|x| \to \infty$.

Next, it is straightforward to see that Eqs. (12) and (13) can be derived from the Lagrangian $\mathfrak{L} = \int_{-\infty}^{+\infty} \mathcal{L}dx$, with density

$$\mathcal{L} = \tfrac{1}{2}U_t^2 + \tfrac{1}{2}w_x^2 + \tfrac{1}{2}U_x w^2 + B_0 U_x w + \tfrac{1}{2}R_0 w^2. \qquad (14)$$

The respective Hamiltonian is $H = \int_{-\infty}^{+\infty} \mathcal{H}dx$, with density

$$\mathcal{H} = \tfrac{1}{2}U_t^2 - \tfrac{1}{2}w_x^2 - \tfrac{1}{2}U_x w^2 - B_0 U_x w - \tfrac{1}{2}R_0 w^2. \qquad (15)$$

To define an effective potential of the interaction of two solitary waves moving with equal velocities v, it is necessary to rewrite Eqs. (12) and (13), together with the Lagrangian and Hamiltonian densities (14) and (15), in the reference frame

moving with velocity v, i.e., in terms of the $\tau = t$ and $\xi = x - vt$ variables, as

$$U_{\tau\tau} - 2vU_{\xi\tau} + v^2 U_{\xi\xi} + \left(\tfrac{1}{2}w^2 + B_0 w\right)_\xi = 0, \qquad (16)$$

$$w_{\xi\xi} - R_0 w - B_0 U_\xi - wU_\xi = 0, \qquad (17)$$

and

$$\mathcal{L}_{\text{moving}} = \tfrac{1}{2}U_\tau^2 - vU_\xi U_\tau + \frac{v^2}{2}U_\xi^2 + \tfrac{1}{2}w_\xi^2$$
$$+ B_0 U_\xi w + \tfrac{1}{2}R_0 w^2 + \tfrac{1}{2}U_\xi w^2, \qquad (18)$$

$$\mathcal{H}_{\text{moving}} = \tfrac{1}{2}U_\tau^2 - \frac{v^2}{2}U_\xi^2 - \tfrac{1}{2}w_\xi^2 - B_0 U_\xi w$$
$$- \tfrac{1}{2}R_0 w^2 - \tfrac{1}{2}U_\xi w^2. \qquad (19)$$

In what follows, we introduce the effective mass M of the solitary wave. In that connection, we note that, in standard models, the solitary wave's kinetic energy, which is produced by the integral, with respect to ξ, of the kinetic part of the Lagrangian density ($\int_{-\infty}^{+\infty} d\xi$), is [20]

$$E_{\text{kin}} = (1/2)Mv^2. \qquad (20)$$

III. THE INTERACTION OF FAR-SEPARATED SOLITARY WAVES

As is customary in studies of generic settings [18,19,21], a pair of interacting solitary waves separated by a large distance L is approximated by juxtaposing two identical solitary-wave solutions given by Eqs. (8) and (7). They interact via their exponentially decaying tails. Assuming that the center of the solitary wave is fixed at $\xi = 0$, and taking into account that $\text{sech}(x) \approx 2e^{-x}$ at $x \to \infty$, the expressions for the tails which are derived by Eqs. (7) and (8) are

$$w_{\text{sol}} \approx \frac{4B_0}{Cv}(v^2 - C^2)\exp\left(-\frac{B_0}{vC}\sqrt{v^2 - C^2}|\xi|\right), \qquad (21)$$

$$u_{\text{sol}} \approx -\frac{B_0}{v^2}w_{\text{sol}} = -\frac{4B_0^2}{Cv^3}(v^2 - C^2)$$
$$\times \exp\left(-\frac{B_0}{vC}\sqrt{v^2 - C^2}|\xi|\right). \qquad (22)$$

In turn, the use of Eq. (11) produces the respective asymptotic expression for the tail of the field U:

$$U_{\text{sol}} \approx \frac{4B_0}{v^2}\sqrt{v^2 - C^2}\,\text{sgn}(\xi)$$
$$\times \exp\left(-\frac{B_0}{vC}\sqrt{v^2 - C^2}|\xi|\right) + c_\pm, \qquad (23)$$

where $c_\pm$ are constant values at $\xi = \pm\infty$. The average value of the asymptotic constants, $(1/2)(c_+ + c_-)$, is arbitrary, while the difference is uniquely determined by the solution as

$$c_+ - c_- = \int_{-\infty}^{+\infty} u_{\text{sol}}(\xi)d\xi. \qquad (24)$$

Next, we consider the pair of solitary waves with centers placed at positions $\xi_0 = \pm L/2$, and the constant value of U

between them [determined by the combination of the corresponding coefficients $c_{\pm}$ in Eq. (23)] set equal to zero, so as to make the configuration symmetric. Then, an effective potential of the interaction between the far-separated solitary waves, $W(L)$, can be derived by means of the general procedure elaborated in Ref. [18]. This is based on the substitution of the juxtaposition of the solitary waves in the expression for H and handling terms with spatial derivatives by means of the integration by parts, so that the actual calculation of the integrals is not necessary, with all the contributions from the integrals being produced by the "surface terms" in the formula for the integration by parts. The result of this procedure is

$$W(L) = \frac{32 B_0^3}{C^3 v^3} (v^2 - C^2)^{5/2} \exp\left(-\frac{B_0}{vC}\sqrt{v^2 - C^2} L\right), \quad (25)$$

with the positive sign of W implying repulsion between the solitary waves. It is relevant to mention that, when calculating the effective potential (25), the result is produced by the third term in the Hamiltonian density (19), while the contributions from the second and fourth ones *exactly cancel each other*. It should be noted here that the connection of the AA system with to the KdV equation at speeds close to C [14] and the pairwise repulsion of KdV solitons [20] are in line with the above analysis.

The repulsion, described above, will lead to a *splitting* of the initially equal velocities of the interacting solitary waves,

$$v \to v \pm \Delta v, \quad (26)$$

provided that Δv represents a small perturbative effect. To obtain Δv from the energy balance, it is necessary to know the exact expression for the energy of individual solitary waves. The substitution of the exact solitary-wave solution given by Eqs. (8) and (7) in the expression for the Hamiltonian, determined by its density (15), leads to a very cumbersome expression. This expression becomes simpler in the limit case when the velocity is taken close to the solitary wave's existence cutoff,

$$v - C \ll C. \quad (27)$$

Then, from Eqs. (7)–(9) we obtain

$$u_{\text{sol}} \approx -\frac{2 B_0^2}{C^3} (v - C) \text{sech}^2\left(\frac{B_0 \sqrt{v - C}}{\sqrt{2} C^{3/2}} \xi\right), \quad (28)$$

$$w_{\text{sol}} \approx \frac{2 B_0}{C} (v - C) \text{sech}^2\left(\frac{B_0 \sqrt{v - C}}{\sqrt{2} C^{3/2}} \xi\right), \quad (29)$$

$$H_{\text{sol}} \approx \frac{8\sqrt{2} B_0^3}{3 C^{5/2}} (v - C)^{3/2}. \quad (30)$$

The consideration of this case is relevant because the exponential smallness in Eq. (25) is less acute for small $(v - C)$. Note, in particular, that the sech^2 limit corresponds to the soliton in the KdV limit of the AA system [14].

Next, the interaction-induced change of the velocities, Δv, is determined by equating the interaction energy (25) to the difference between the energy of the two-solitary-wave configuration and the sum of individual energies of the two

solitary waves, with the velocities split as per Eq. (26):

$$\Delta(H_{\text{two sol.}}) \approx \frac{\partial^2 H_{\text{sol}}}{\partial v^2} (\Delta v)^2 \approx \frac{2\sqrt{2} B_0^3}{C^{5/2} \sqrt{v - C}} (\Delta v)^2, \quad (31)$$

where condition (27) is used to simplify the expression, as it follows from Eq. (30). Finally, equation $\Delta(H_{\text{two sol.}}) = W(L)$ yields the result, which is valid under condition (27), provided that the result also satisfies the constraint $\Delta v \ll v - C$ (i.e., it is a small perturbative effect):

$$\Delta v \approx \frac{8}{\sqrt{C}} (v - C)^{3/2} \exp\left(-\frac{B_0 \sqrt{v - C}}{\sqrt{2} C^{3/2}} L\right). \quad (32)$$

Note that, for fixed large L and fixed C and B_0, the interaction-induced velocity change Δv, as given by Eq. (32) and considered as a function of $(v - C)$, attains a maximum (the strongest perturbative effect of the interaction) at

$$(v - C)|_{\text{max}} = 18 C^3 / (B_0 L)^2, \quad (33)$$

the maximum value itself being

$$(\Delta v)_{\text{max}} = \left(\frac{6\sqrt{2}}{e}\right)^3 \frac{C^4}{(B_0 L)^3} \approx 30 \frac{C^4}{(B_0 L)^3}. \quad (34)$$

The above calculation, albeit approximate (especially since the velocity difference will keep changing as separation L changes), suggests an important qualitative observation that is corroborated below by numerical computations. In particular, if we start from a symmetric configuration, it will progressively become asymmetric, leading to a pattern with a taller and faster solitary wave on the right and a shorter, slower solitary wave on the left. Below it is confirmed that, indeed, such a configuration in terms of heights and speeds is formed in the case of multi-solitary-wave states.

In a quantitative form, the relative motion of interacting solitary waves obeys the dynamical equation

$$\frac{d^2 L}{d\tau^2} = -\frac{1}{M_{\text{reduced}}} \frac{dW}{dL}. \quad (35)$$

Here, the reduced mass M_{reduced} of the solitary-wave pair is considered to be

$$M_{\text{reduced}} = (1/2) M, \quad (36)$$

where we have adopted the particlelike nature of the solitary wave, together with the standard result of the classical mechanics concerning the interaction of two point masses; thus, in Eq. (36), M represents the abovementioned mass of a single solitary wave [see Eq. (20)]. Actually, the calculation of M is a central point in our analysis, as concerns the comparison with numerical results (see the next section and Appendix B). We also note that the above approach to the prediction of the evolution of the separation between the solitary waves is based on the energetics of the multi-solitary-wave ansatz. A systematic analysis, including all the associated technical details at the level of the PDE system and conservation laws, generalizing another approach, introduced by Manton [19], is presented in Appendix A. We demonstrate that it leads to the same result as Eq. (35), thus confirming the above findings.
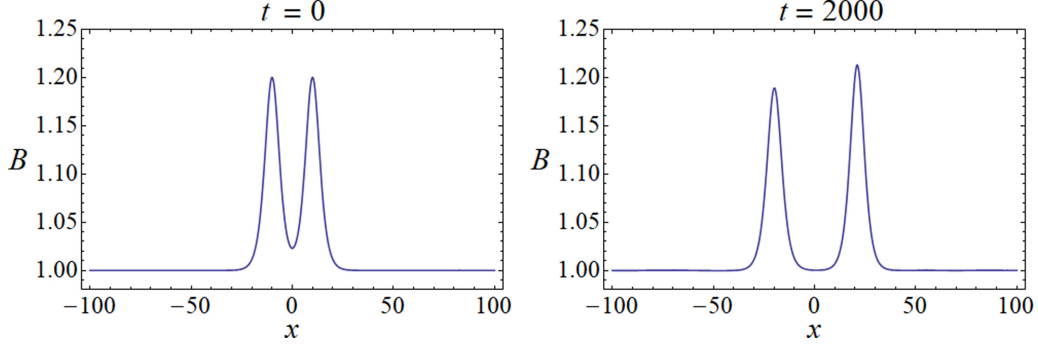
FIG. 1. Results of simulations of the interaction of two solitary waves, as they are observed in the co-traveling reference frame for initial velocities $v_{1,2}(t = 0) = 1.1$ and positions $x_{1,2}(t = 0) = \pm 10$. The two solitary waves, which initially have equal velocities, end up with different ones and, consequently, unequal heights.

IV. NUMERICAL RESULTS

A. The simulations

To perform a numerical study of the dynamics of interacting solitary waves in the AA model, we first consider a pair of solitary waves with equal velocities,

$$v_{1,2}(t = 0) = 1.1, \qquad (37)$$

which are initially placed at $x_{1,2}(t = 0) = \pm 10$, i.e., the initial distance between them is $L(0) = x_1(t = 0) - x_2(t = 0) = 20$. In all simulations, we set $B_0 = R_0 = 1$ (for this choice, the dimensionless form of the AA model considered here coincides with the one adopted in Ref. [15]), which means $C = 1$ [see Eqs. (1)–(3)]. To apply the numerical method, the spatial variable was discretized by finite differences, and forward marching in time was performed. The finite-difference scheme in space was implemented taking into regard the coupling of a given site with second neighbors, in order to produce a stable numerical algorithm. The time integration has been performed with the Runge-Kutta method of the 4th–5th order. To check the precision of the results, we used, as a diagnostic, the value of the total energy of the system calculated according to Eq. (15). Relative variance of the energy in all the simulations was $< 10^{-6}$.

Since the physically relevant interval of the solitary waves' velocities is, according to Eq. (10), $1 < v < 2$, the selected value (37) is close to the lower edge of the interval. As can be inferred from Eqs. (8) and (7), the solitary waves in this velocity region are wide, which implies that their interaction is stronger; as a result, shorter integration times are required so that the interaction manifest itself.

The dynamical behavior of the two interacting solitary waves, in the co-traveling reference frame, is shown in Fig. 1. The symmetric configuration is quickly converted into one in which one solitary wave becomes taller (and consequently quicker) than the other. This is expected, as predicted by the analysis of the previous section, since the repelling interaction of the solitary waves causes a change in their velocities, $\Delta v_1 > 0$ and $-\Delta v_2 < 0$, so that the velocities resulting from the interaction are

$$v_1 = v_1(t = 0) + \Delta v_1 > v_2 = v_2(t = 0) - \Delta v_2. \qquad (38)$$

The situation is reversed when we consider initial velocities with the opposite sign; in this case, the resulting configuration is a mirror image of Fig. 1 (not shown here).

Similar phenomenology is observed in the simulations if we consider more than two solitary waves placed symmetrically, with equal initial velocities. In particular, in Fig. 2 we display a four-solitary-wave configuration. In this case, the result shows a graded configuration of increasingly taller and faster solitary waves, which keep separating from each other in the course of the subsequent evolution.

In addition, we have considered the evolution of solitary-wave sets with higher initial velocities (equal for all the pulses in the set, and with the same initial distance between them), taken in the range of $1.25 \leqslant v(t = 0) \leqslant 1.9$. We observed the same phenomenology but, as the width of the waves becomes smaller with the increase of v, the interaction becomes, accordingly, weaker and the corresponding dynamical response is slower than in the above case of $v(t = 0) = 1.1$.

B. Comparison of the analytical estimate with numerical simulations

From the predicted form of the interaction potential (25) and expression (36) for the reduced mass, we derive the equation of motion for the distance between the two solitary waves:

$$\frac{d^2 L}{d\tau^2} = -\frac{2}{M}\frac{d}{dL}W(L) = \frac{2A(v)}{M}\exp{(-\lambda L)}, \qquad (39)$$

where

$$A(v) \equiv \frac{32B_0^4}{C^4 v^4}(v^2 - C^2)^3, \quad \lambda \equiv \frac{B_0}{vC}\sqrt{v^2 - C^2}. \qquad (40)$$

A subtle issue in this connection is the identification of the mass M of the solitary wave. Considering either the kinetic energy term in the Hamiltonian (for a stationary solitary wave in the co-traveling reference frame), and setting it equal to $(1/2)Mv^2$, or the momentum

$$P = -\int_{-\infty}^{+\infty} U_t U_x\, dx, \qquad (41)$$

and setting it equal to Mv, leads to the conclusion that

$$M = \int_{-\infty}^{+\infty} u^2\, dx. \qquad (42)$$

In Appendix B we further explore this definition of the solitary wave's mass, upon considering the dynamical response of
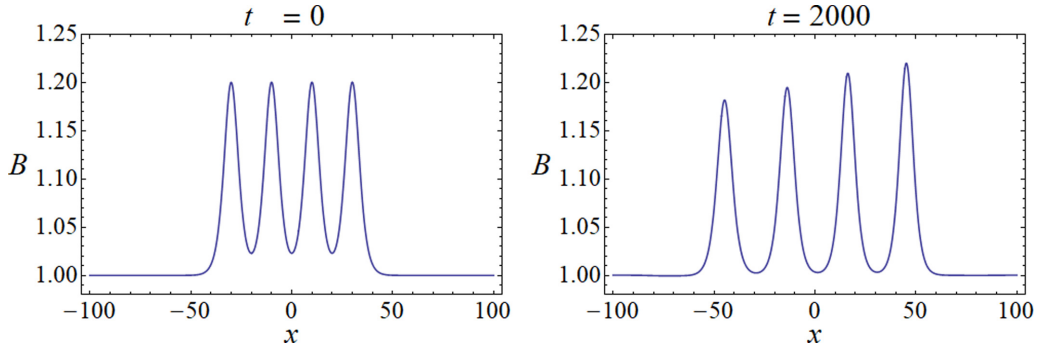
FIG. 2. The result of the simulation of the set of four interacting solitary waves in the co-traveling reference frame. The initial velocities are $v_{1,2,3,4}(0) = 1.1$, and their initial positions are $x_{1,4}(0) = \pm 30$ and $x_{2,3}(0) = \pm 10$. The solitary waves end up with different velocities and, consequently, different heights (cf. Fig. 1).

the solitary wave to a perturbation represented by a potential term added to the system, which is also corroborated by direct numerical simulations.

Here it should be pointed out that the above expression for M is not an intuitively evident one, as it refers solely to the mass associated with the u component of the AA solitary wave, while the w component does not contribute to the calculation of the mass, because Eq. (6) for this component does not contain time derivatives. In light of this fact, here we proceed in the following way: by numerically solving the ordinary differential equation (ODE) (39), we obtain the distance L between the two solitary waves as a function of time. This prediction is compared to the full numerical result, produced by simulations of the AA system, i.e., Eqs. (5) and (6). Assuming that the tail-tail interaction force, produced by both the energetic considerations and the Manton method (see Appendix A), adequately characterizes the exponential nature of the pairwise repulsion between the solitary waves, we then use the above semianalytical prediction and its comparison to the full numerical results to "adjust" the proper expression for the mass. This approach reveals a relevant correction to the effective mass of the solitary wave.

As said above, we aim, first, to numerically integrate Eqs. (5) and (6) and thus obtain the distance between the interacting solitary waves as a function of time. For this purpose, we use velocities $v \geqslant 1.5$, to make the waves more well-separated and thus improve the accuracy of the comparison of the full numerical results with predictions of the ODE (39), where the constants and the "naively defined" solitary wave's mass are taken as per Eqs. (40) and (42), respectively. The results for $v = 1.6$ are shown in Fig. 3, where the red solid and dashed blue lines show, respectively, the distance between the solitary waves, as obtained from the direct numerical integration of Eqs. (5) and (6) and predicted by the solution of the ODE (39). In this case, the discrepancy between the PDE and ODE results is obvious. Similar results are produced by the comparison at other values of the parameters.

Following the path outlined above, we attribute the discrepancy to the uncertainty regarding the solitary wave's mass. To fix the issue, we "phenomenologically" incorporate a fitting factor $\alpha(v)$ in Eq. (39), rewriting it as

$$\frac{d^2L}{d\tau^2} = \frac{A(v)}{M^*_{\text{reduced}}} \exp(-\lambda L), \quad \text{with } M^*_{\text{reduced}} = \frac{M}{2\alpha(v)}. \quad (43)$$

Then, we determine the value of $\alpha(v)$ required for the PDE- and ODE-produced curves to match. The results are shown, for $v = 1.6$ and other values of the initial velocities, in Fig. 4 and Table I. In particular, for $v = 1.6$ the two curves are made virtually identical by dint of the adjustment factor $\alpha = 0.3045$ in Eq. (43). This observation and similar findings for other initial velocities confirm that the above analysis correctly captures the exponential decay of the inter-solitary-wave repulsive force, yet the straightforward theory misses the right prefactor in the respective equation of motion (39). In this connection, we stress that, for our analysis to be relevant for the comparison to the full simulations, we need the solitary waves to be well separated, in order to apply the assumption of the tail-to-tail interaction, but not too far from each other either, lest the integration time, needed to make the interaction effect tangible, be extremely large. In the present setting, we considered the initial separation of $L(0) = 20$, and we did not observe any significant difference in the accuracy of the obtained results for larger separations.

To summarize these results, we sought a function $\alpha = \alpha(v)$ which may fit the data from Table I. As it is seen in the
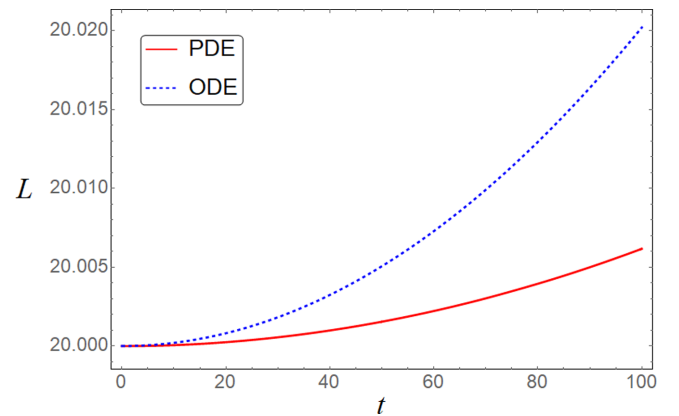

FIG. 3. The comparison of the results for the distance L between the two interacting solitary waves in the co-traveling reference frame, for initial velocities $v_{1,2}(0) = 1.6$. The (red) solid and (blue) dashed lines present the results produced by direct simulations of the underlying PDEs (5) and (6) and by the numerical solution of the effective ODE (39) with the constants taken as per Eqs. (40) and (42).
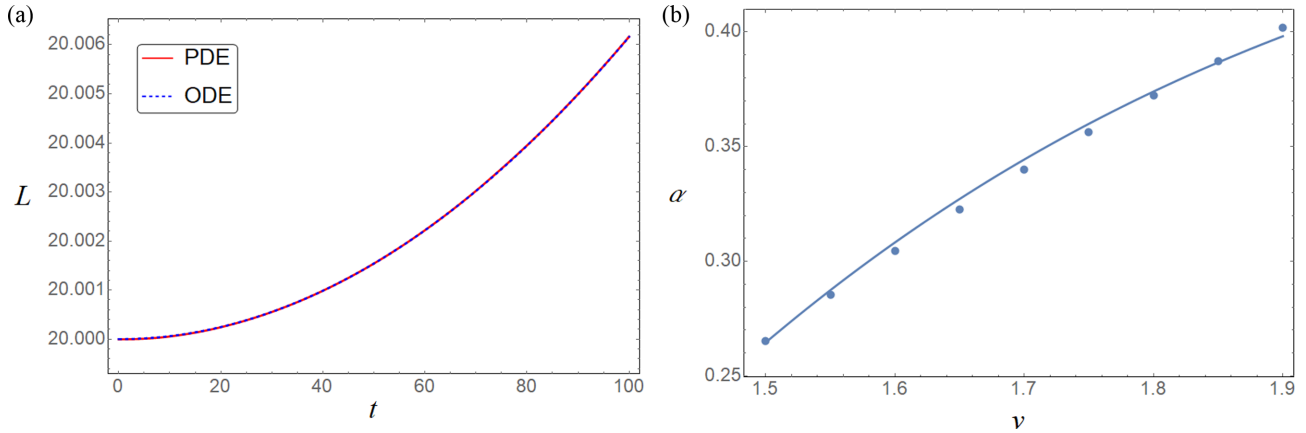
FIG. 4. Panel (a) shows the comparison between the PDE results [solid (red) curve], the same as in Fig. 3), for the distance $L(t)$ between the interacting solitary waves in the co-traveling reference frame, and the ODE counterpart [dashed (blue) curve], produced by Eq. (43) using the fitting prefactor $\alpha = 0.3045$, in the case of $v_{1,2}(0) = 1.6$. It is seen that this value of 2α makes the two curves practically identical. Panel (b) shows, by means of the chain of dots, the fitting half-factor α for different values of the initial speed, as per the data presented in Table I. The continuous curve plots an interpolating function (44), which approximates the values of $\alpha(v)$.

Fig. 4(b), a reasonable choice is

$$\alpha(v) = 1.05(v^2 - C^2)^2/v^{9/2}. \tag{44}$$

This function is built as a combination of powers of $(v^2 - C^2)$ and v, as these factors naturally appear in the calculation of the interaction force for the solitary waves. In Appendix B, we evaluate the relevance of considering the variation of the solitary wave's mass in the context of the solitary-wave–defect interaction.

V. CONCLUSIONS

In the present work, we have revisited the Adlam-Allen (AA) model, governing the propagation of solitary waves in cold magnetized collisionless plasmas, in the presence of the electric field (in addition to a magnetic field). The AA model is one of the fundamental nonlinear models of plasma physics [8,11–13] that has made the prediction of solitary waves possible, well before the (re)discovery of the KdV equation and its celebrated solitons in the framework of the Fermi-Pasta-Ulam-Tsingou model. Indeed, the AA system is a source of localized and periodic waves, not only in the context of the transverse magnetic field applied to the plasmas but also more recently for a longitudinal field [27,28].

Here, we have studied the interaction between solitary waves, a theme of substantial interest in the theory of solitary waves and solitons [18–20]. We provide the energy analysis, based on the Hamiltonian structure of the model, and complement it with a detailed derivation of the same result by means of an alternative (Manton's) method (see Appendix A). The resulting Newtonian dynamics for the separation clearly reveals the repulsive character of the interaction, as well as the exponential dependence of the force on the separation.

This is natural to expect near the lower edge of the range (10) of accessible solitary wave speeds, where the model is close to the KdV limit (as shown earlier in Refs. [14,15]) and, thus, inherits the repulsive interaction between solitons which is well known in the framework of the KdV equation. Nevertheless, an essential element of uncertainty remains in the form of an accurate expression for the effective mass of the two-component solitary wave. We have side-stepped this uncertainty by finding a suitable velocity-dependent fitting factor, which takes values, roughly, between $2\alpha = 0.5$ and 0.8, which depends on the wave's speed. This prefactor secures the full match between the ODE (semianalytical) and PDE (fully numerical) results for the separation between the interacting solitary waves.

While our analysis provides a definitive explanation for the exponentially repulsive nature of the interactions, a remaining intriguing issue concerns the speed-dependent prefactor in the respective effective equation of motion for the separation between the interacting solitons. This amounts to an effective renormalization of the solitary wave's dynamic mass. The same issue also concerns the dynamics of the soliton gas in the AA system. A prototypical example of the latter was demonstrated in Fig. 2 for a configuration consisting of four interacting solitary waves, initially having equal velocities, which end up with different velocities and, consequently, different heights. This issue may also be relevant for other effectively nonlocal systems, in which one equation does not contain time derivatives (e.g., a Poisson-like equation). Systems of the latter type arise, in particular, in models of thermal media, plasmas, nematic liquid crystals, and Bose-Einstein condensates (see recent examples in Refs. [29,30] and references therein). Such systems, as well as higher-dimensional plasma models, are natural platforms for future

TABLE I. Values of the fitting half-factor α in Eq. (43) which provide the best match of $L(t)$ to the results of PDE simulations at different values of v.

v	1.5	1.55	1.6	1.65	1.7	1.75	1.8	1.85	1.9
α	0.2653	0.2855	0.3045	0.3227	0.34	0.3565	0.3724	0.3874	0.4019

work. Progress along these directions will be reported elsewhere.

APPENDIX A: DERIVATION OF THE POTENTIAL OF THE SOLITARY WAVES' INTERACTION VIA MANTON'S APPROACH

Here, we aim to derive the interaction potential (25) by means of another approach, namely, upon following the Manton method [19].

Introducing the traveling coordinate ξ, as per Eq. (9), in Eqs. (12) and (13) we obtain

$$U_{\tau\tau} - 2vU_{\xi\tau} + v^2 U_{\xi\xi} + B_0 w_\xi + \tfrac{1}{2}(w^2)_\xi = 0, \qquad \text{(A1)}$$

$$w_{\xi\xi} - R_0 w - B_0 U_\xi - U_\xi w = 0. \qquad \text{(A2)}$$

In the context of Klein-Gordon equations, the Manton method explores the evolution of momentum P (as its time derivative is associated with the force, which here stems solely from the inter-solitary-wave interaction) [19]. The expression for the field momentum in the co-moving frame is given by

$$\tilde{P} = \int_{-\infty}^{+\infty} U_\tau U_\xi \, d\xi. \qquad \text{(A3)}$$

Differentiating the above expression momentum in time, we obtain

$$
\begin{aligned}
\frac{d\tilde{P}}{d\tau} &= -\int_{-\infty}^{+\infty} (U_{\tau\tau} U_\xi + U_\tau U_{\xi\tau}) d\xi \\
&= -\int_{-\infty}^{+\infty} \left[\left(2vU_{\xi\tau} - v^2 U_{\xi\xi} - B_0 w_\xi - \tfrac{1}{2}(w^2)_\xi \right) U_\xi + U_\tau U_{\xi\tau} \right] d\xi \\
&= \int_{-\infty}^{+\infty} \left[(B_0 + w) w_\xi U_\xi - \tfrac{1}{2}\left(U_\tau^2\right)_\xi - v\left(U_\xi^2\right)_\tau + \tfrac{1}{2}v^2\left(U_\xi^2\right)_\xi \right] d\xi.
\end{aligned}
\qquad \text{(A4)}
$$

In line with the original approach of Ref. [19], we proceed by considering two well-separated solitary waves, one placed at $x = 0$ and the other one at $x = L \gg 0$. We also set two points, $x = a$ and $x = b$, with $a \to -\infty$ and $0 \ll b \ll L$. Next, following Ref. [19], we neglect the two middle terms in the above equation, as we consider quasistationary solutions, and by using (12) we get

$$
\begin{aligned}
\frac{d\tilde{P}}{dt} &= -\int_a^b \left[(R_0 w - w_{\xi\xi}) w_\xi - \frac{v^2}{2}(u^2)_\xi \right] d\xi \\
&= \left[\frac{1}{2} w_\xi^2 - \frac{1}{2} R_0 w^2 + \frac{v^2}{2} u^2 \right]_a^b.
\end{aligned}
\qquad \text{(A5)}
$$

Now, we consider the superposition ansatz for the far-separated solitary waves, $w = w_1 + w_2$. We use the fact that the decay of the tails of the solitary waves is exponential. Thus, the contributions at $x = a$ vanish, while those at $x = b$ are of the following forms:

$$w_1 \sim e^{-\lambda\xi} \quad \text{and} \quad w_2 \sim e^{\lambda(\xi - L)}. \qquad \text{(A6)}$$

Then, the contributions in Eq. (A5), which are mixed (and consequently account for the interaction), are at point $x = b$:

$$\frac{d\tilde{P}}{d\tau} = w_{1_\xi} w_{2_\xi} - R_0 w_1 w_2 + v^2 u_1 u_2. \qquad \text{(A7)}$$

The asymptotic forms (21) and (22) yield

$$
\left.
\begin{aligned}
w_1 &\approx \frac{4B_0}{Cv}(v^2 - C^2)e^{-\lambda\xi} \\
w_2 &\approx \frac{4B_0}{Cv}(v^2 - C^2)e^{\lambda(\xi - L)}
\end{aligned}
\right\}
\Rightarrow
\quad
\begin{aligned}
w_{1\xi} &\approx -\frac{4B_0^2}{C^2 v^2}(v^2 - C^2)^{3/2} e^{-\lambda\xi}, \\
w_{2\xi} &\approx \frac{4B_0^2}{C^2 v^2}(v^2 - C^2)^{3/2} e^{\lambda(\xi - L)},
\end{aligned}
\qquad \text{(A8)}
$$

and

$$
\begin{aligned}
u_1 &\approx -\frac{4B_0^2}{Cv^3}(v^2 - C^2)e^{-\lambda\xi}, \\
u_2 &\approx -\frac{4B_0^2}{Cv^3}(v^2 - C^2)e^{\lambda(\xi - L)},
\end{aligned}
\qquad \text{(A9)}
$$

with $\lambda = (B_0/Cv)\sqrt{v^2 - C^2}$. Thus, by also using $R_0 = B_0^2/C^2$, Eq. (A7) reads

$$\frac{d\tilde{P}}{d\tau} = -\frac{16B_0^4}{C^4v^4}(v^2 - C^2)^3 e^{-\lambda L} - \frac{16B_0^4}{C^4v^2}(v^2 - C^2)^2 e^{-\lambda L}$$
$$+ \frac{16B_0^4}{C^2v^4}(v^2 - C^2)^2 e^{-\lambda L}, \tag{A10}$$

or

$$\frac{d\tilde{P}}{d\tau} = -\frac{32B_0^4}{C^4v^4}(v^2 - C^2)^3 e^{-\lambda L}. \tag{A11}$$

Then, according to Eq. (35), we get

$$\frac{d^2L}{d\tau^2} = \frac{1}{M_{\text{reduced}}}\frac{32B_0^4}{C^4v^4}(v^2 - C^2)^3 e^{-\lambda L}. \tag{A12}$$

For the potential, we get

$$W(L) = \frac{32B_0^3}{C^3v^3}(v^2 - C^2)^{5/2} e^{-\lambda L}. \tag{A13}$$

These expressions recover the results that were obtained in the main text via the energetic arguments [Eq. (25)] and thus corroborate the repulsive exponentially decaying interaction between the solitary waves, mediated by their tails.

APPENDIX B: INTERACTION OF THE SOLITARY WAVE WITH A PARAMETRIC FORCE

Our aim in the present Appendix is to study the interaction between a solitary wave of the system with a defect using Manton's approach and to assess the relevance of mass variation during such an interaction. To do so, we introduce a perturbation term F in Eq. (5) as follows:

$$u_{tt} + \left(\tfrac{1}{2}w^2 + B_0w\right)_{xx} = F, \quad \text{with } F \equiv f(x)u(x,t). \tag{B1}$$

The reasoning behind this choice of perturbation and the form of $f(x)$ is the following. Arguably, one of the simplest possibilities is to define a spatially localized parametric drive which introduces a small localized perturbation to the motion of the solitary wave and is compatible with the zero boundary conditions as $x \to \pm\infty$ (in fact, as $x \to \pm\tilde{L}/2$, where $\tilde{L}$ is the size of the integration domain). In particular, we select

$$f \equiv f_0 \frac{\sinh(x/l)}{\cosh^3(x/l)}. \tag{B2}$$

Here f_0 and l characterize, respectively, the amplitude and the width of the spatially localized parametric perturbation term. In the subsequent numerical investigation, we considered a solitary wave with velocity $v_0 = 1.7$, under the action of the perturbation of the above form, with $f_0 = 0.1$ and $l = 1.5$.

To utilize Manton's approach, we use the system's equation of motion written in terms of field w, potential U, and the co-traveling coordinates (ξ, τ). This way the system becomes

$$U_{\tau\tau} - 2vU_{\xi\tau} + v^2U_{\xi\xi} + B_0w_\xi + \frac{1}{2}(w^2)_\xi = \int_{-\infty}^{\xi} f\frac{\partial U}{\partial\xi'}d\xi'. \tag{B3}$$
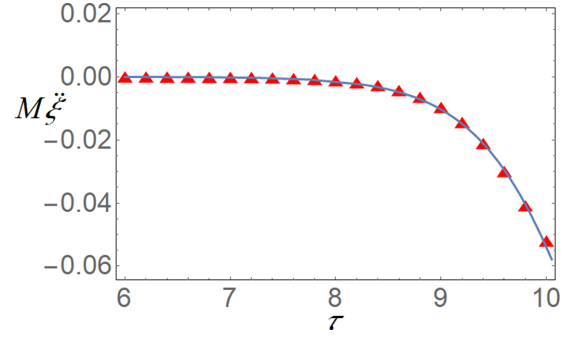

FIG. 5. Comparison of the right-hand sides of Eqs. (B6) and (B8). The blue solid line and the chain of red triangles depict, respectively, the right-hand sides of Eqs. (B6) and (B8).

We recall that the momentum of the soliton in the moving frame is given by

$$\tilde{P} = -\int_{-\infty}^{+\infty} U_\tau U_\xi \, d\xi, \tag{B4}$$

and its derivative is given by

$$\frac{d\tilde{P}}{d\tau} = -\int_{-\infty}^{+\infty} U_{\tau\tau}U_\xi \, d\xi - \int_{-\infty}^{+\infty} U_\tau U_{\xi\tau} \, d\xi. \tag{B5}$$

By substituting the $U_{\tau\tau}$ term from Eq. (B3) into Eq. (B5), we obtain

$$\frac{d\tilde{P}}{d\tau} = -2v\int_{-\infty}^{+\infty} U_{\xi\tau}U_\xi \, d\xi + v^2\int_{-\infty}^{+\infty} U_{\xi\xi}U_\xi \, d\xi$$
$$+ \int_{-\infty}^{+\infty}\left[B_0w_\xi + \frac{1}{2}(w^2)_\xi\right]U_\xi \, d\xi$$
$$- \int_{-\infty}^{+\infty} U_\xi \int_{-\infty}^{\xi} f\frac{\partial U}{\partial\xi'}d\xi' \, d\xi - \int_{-\infty}^{+\infty} U_\tau U_{\xi\tau} \, d\xi. \tag{B6}$$

On the other hand, we assume that $U = U[\xi - \xi_0(\tau)]$, which represents a traveling-wave solution with its (moving) center $\xi_0(\tau)$. This is the only essential assumption adopted for the current analysis; i.e., we are exploring the dynamics of an adiabatically varying solitary wave whose properties are slowly varying in the presence of the defect. Thus, we set $U_\tau = -U_\xi \dot{\xi}_0$, where $\dot{\xi}_0 = \frac{d\xi_0}{d\tau}$, and from Eq. (B4) we get, also using definition (42),

$$\tilde{P} = \dot{\xi}_0\int_{-\infty}^{+\infty} U_\xi^2 \, d\xi = \dot{\xi}_0\int_{-\infty}^{+\infty} u^2 \, d\xi = \dot{\xi}_0 M \tag{B7}$$

and, accordingly,

$$\frac{d\tilde{P}}{d\tau} = M\ddot{\xi}_0 + \dot{M}\dot{\xi}_0. \tag{B8}$$

The right-hand sides of Eqs. (B6) and (B8) should match. Indeed, if we consider the numerical solution of the system for U and w, as well as the calculated mass M, we see in Fig. 5 that they match. Note that we only consider the evolution up to $\tau = 10$, rather than the full time interval of the interaction between the solitary wave and the potential. This is done because when the solitary wave interacts fully with the defect, it is deformed (as it can be
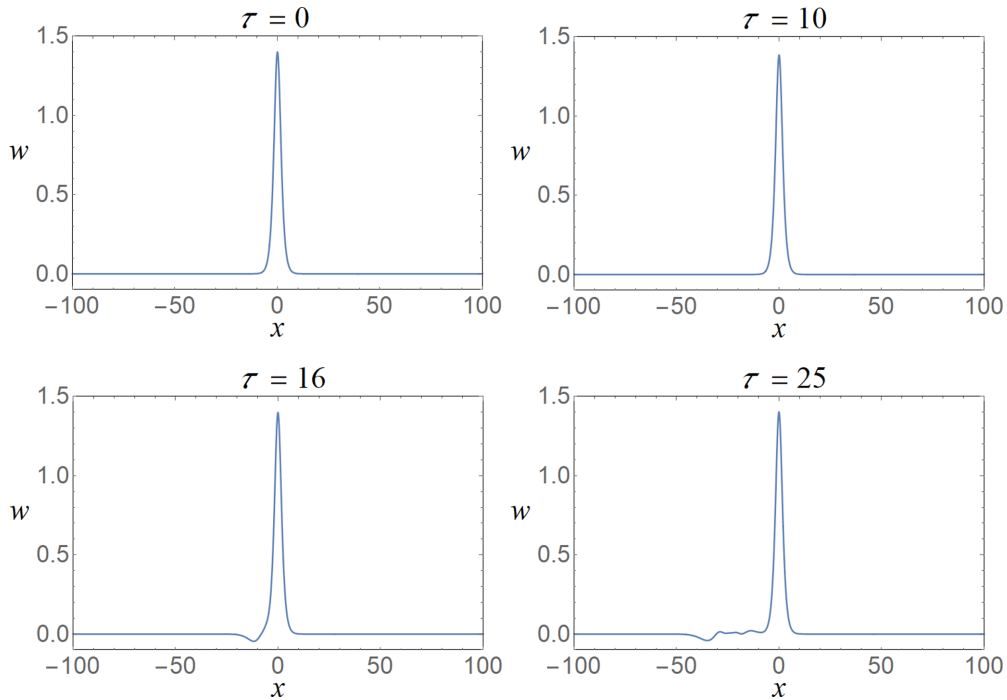
FIG. 6. The interaction of the solitary wave with $v = 1.7$ with the localized inhomogeneity introduced by Eq. (B1) in the co-moving frame. The inhomogeneity is initially set at $x = 20$. Up to $\tau = 10$, the form of the wave remains practically intact. At $\tau = 16$ we observe deformation of the wave, and at $\tau = 25$ we observe the emergence of a small-amplitude shelf which, along with the accompanying tail, is attached to the (primary) solitary wave.

seen in Fig. 6 for $\tau = 16$) and the adiabatic-traveling-wave assumption is no longer valid, broken by the emission of radiation, as observed in the bottom panels of Fig. 6. On the other hand, up to $\tau = 10$ it is relevant to assume that only the tail of the solitary wave and the defect's potential interact, the shape of the wave being only adiabatically modified, in line with the underlying assumptions. In Fig. 6, we consider the evolution in the co-moving frame, and thus the main body of the solitary wave appears still, while the inhomogeneity moves with negative velocity $v' = -1.7$.

Let us now evaluate terms contributing to the change of the momentum in the force balance associated with this problem. The contribution of the $\dot{M}\dot{\xi}_0$ term in Eq. (B8) turns out to be negligible in comparison with the $M\ddot{\xi}_0$ one, being at least 2 orders of magnitude smaller than the latter one. For example, for $\tau^* = 9.5$ we have $M(\tau^*)\ddot{\xi}_0(\tau^*) = -0.025\,122\,9$ and $\dot{\xi}_0(\tau^*)\dot{M}(\tau^*) = 0.000\,109\,553$. Notice that in this setting the mass is evaluated to be $M(\tau^*) = 1.714\,875\,5$, the accel-

eration is $\ddot{\xi}(\tau^*) = -0.014\,65$, and the arising change in the mass is characterized by $\dot{M}(\tau^*) = -0.014\,710\,1$ and $\dot{\xi}(\tau^*) = -0.025\,122\,9$. It is thus concluded that, in the course of the time interval where this Manton-type method force balance is applicable, the variation of the mass is explicitly estimated to be $\approx 1\%$ in comparison to the actual solitary-wave mass; hence, for the time interval of our current considerations, the mass change does not substantially affect the wave-defect interaction.

Naturally, there remains an important open question whether the mass-fitting factor, used for the analysis of the solitary-wave collisions, has some extension or connection to the mass variation in the wave-defect interaction. However, given the different nature of the two interactions (and the fact that we can only pursue the solitary-wave interaction until the substantial emission of radiation occurs, as explained in Figs. 5 and 6), this issue stays outside the purview of the present work.

[1] E. Infeld and G. Rowlands, *Nonlinear Waves, Solitons and Chaos* (Cambridge University Press, Cambridge, 1990).

[2] M. Kono and M. M. Skorić, *Nonlinear Physics of Plasmas* (Springer-Verlag, Heidelberg, 2010).

[3] N. J. Zabusky and M. D. Kruskal, Phys. Rev. Lett. **15**, 240 (1965).

[4] E. Fermi, J. Pasta, and S. Ulam, Technical Report Los Alamos National Laboratory LA1940, 1955.

[5] T. Dauxois, Phys. Today **61**(1), 55 (2008).

[6] D. J. Korteweg and G. de Vries, Philos. Mag. **39**, 422 (1895).

[7] H. Washimi and T. Taniuti, Phys. Rev. Lett. **17**, 996 (1966).

[8] J. E. Allen, Phys. Scr. **57**, 436 (1998).

[9] M. Remoissenet, *Waves Called Solitons* (Springer, Berlin, 1999).

[10] M. J. Ablowitz, *Nonlinear Dispersive Waves: Asymptotic Analysis and Solitons* (Cambridge University Press, Cambridge, 2011).

[11] J. H. Adlam and J. E. Allen, Philos. Mag. **3**, 448 (1958).

[12] J. H. Adlam and J. E. Allen, Proc. Phys. Soc. **75**, 640 (1960).

[13] J. E. Allen and J. Gibson, Phys. Plasmas **24**, 042106 (2017).

[14] J. E. Allen, D. J. Frantzeskakis, N. I. Karachalios, P. G. Kevrekidis, and V. Koukouloyannis, Phys. Rev. E **102**, 013209 (2020).

[15] C. M. C. Nairn, R. Bingham, and J. E. Allen, J. Plasma Phys. **71**, 631 (2005).

[16] G. B. Whitham, *Linear and Nonlinear Waves* (Wiley, New York, 1974).

[17] R. J. LeVeque, SIAM J. Appl. Math. **47**, 254 (1987).

[18] B. A. Malomed, Phys. Rev. E **58**, 7928 (1998).

[19] N. S. Manton, Nucl. Phys. B **150**, 397 (1979).

[20] Yu. S. Kivshar and B. A. Malomed, Rev. Mod. Phys. **61**, 763 (1989).

[21] P. G. Kevrekidis, A. Khare, and A. Saxena, Phys. Rev. E **70**, 057603 (2004).

[22] N. Meyer-Vernet, *Basics of the Solar Wind* (Cambridge University Press, Cambridge, 2007).

[23] D. G. Swanson, *Plasma Waves* (Academic Press, London, 1989).

[24] T. H. Stix, *Waves in Plasmas* (Springer-Verlag, New York, 1992).

[25] L. Davis, R. Lüst, and A. Schlüter, Z. Naturforsch. A **13**, 916 (1958).

[26] B. A. Malomed, D. Anderson, M. Lisak, M. L. Quiroga-Teixeiro, and L. Stenflo, Phys. Rev. E **55**, 962 (1997).

[27] G. Abbas, J. E. Allen, M. Coppins, L. Simons, and L. James, Phys. Plasmas **27**, 042102 (2020).

[28] G. Abbas, P. G. Kevrekidis, J. E. Allen, V. Koukouloyannis, D. J. Frantzeskakis, and N. Karachalios, J. Phys. A: Math. Theor. **53**, 425701 (2020).

[29] T. P. Horikis and D. J. Frantzeskakis, Phys. Rev. Lett. **118**, 243903 (2017).

[30] J. Qin, Z. Liang, B. A. Malomed, and G. Dong, Phys. Rev. A **99**, 023610 (2019).